



Providing Choice & Value
Generic CT and MRI Contrast Agents

**FRESENIUS
KABI**

CONTACT REP

AJNR

First Results in an MR Imaging-Compatible Canine Model of Acute Stroke

A. Shaibani, S. Khawar, W. Shin, T.A. Cashen, B. Schirf, M. Rohany, S. Kakodkar and T.J. Carroll

AJNR Am J Neuroradiol 2006, 27 (8) 1788-1793
<http://www.ajnr.org/content/27/8/1788>

This information is current as
of July 20, 2025.

ORIGINAL RESEARCH

A. Shaibani
S. Khawar
W. Shin
T.A. Cashen
B. Schirf
M. Rohany
S. Kakodkar
T.J. Carroll

First Results in an MR Imaging-Compatible Canine Model of Acute Stroke

BACKGROUND AND PURPOSE: The purpose of this work was to develop an MR imaging-compatible animal model of reversible embolic stroke. We hypothesize that real-time MR imaging of the brain can be performed during stroke thrombolysis and can provide real-time feedback and guidance on the success of thrombolysis.

METHODS: Embolic strokes were induced in 5 adult dogs by the use of autologous blood clots, with a sixth dog serving as an experimental control. Serial MR anatomic and physiologic imaging was performed to track the evolution of the stroke. The apparent diffusion coefficient (ADC) and quantitative cerebral blood flow (qCBF) were compared in the normal and stroke regions. During and after the administration of a chemical thrombolytic agent, MR imaging was performed to assess the outcome of the treatment.

RESULTS: Strokes were successfully created in 5 animals. No ADC or qCBF changes were observed in the control animal. Both ADC and qCBF values were found to be significantly different in the region affected by the stroke. Restoration of flow was observed in 1 case.

CONCLUSION: We have successfully implemented an MR imaging-compatible canine model of reversible embolic stroke.

Stroke is the third leading cause of death in the United States, with estimates of death and disability ranging from 500,000 to 731,000 annually.^{1,2} The goal of current imaging and diagnosis of stroke is to identify brain tissue that is hypoperfused but salvageable, the so-called “ischemic penumbra.” An effective means to reduce the neurologic deficit from stroke is to restore blood flow to the ischemic penumbra. In a number of multicenter trials, thrombolysis has been shown to be successful at restoring blood flow.^{3–6} However, a high rate of cerebral hemorrhage (10%–15%) has prompted the Food and Drug Administration to limit the use of IV thrombolytic therapy to within 3 hours of onset of symptoms. The restrictive 3-hour time window limits the administration of thrombolytic agents to only 1%–2% of patients presenting with acute ischemic stroke.^{7,8} Extending this window of opportunity for thrombolysis by identifying those patients who would still benefit from thrombolysis is an active area of research worldwide.

The utility of any treatment that intends to extend the treatment window, or study alternative approaches to chemical thrombolysis, must be evaluated in a realistic and reproducible model of acute stroke. We report on the implementation of a canine model of reversible acute stroke using autologous blood clots.^{9,10} The rationale for conducting these experiments in a canine model are several. First, to achieve optimal resolution for MR imaging techniques, the subject brain has to be larger than that found in rodent or feline models. Second, the canine model is well established for the study of cerebrovascular diseases such as stroke and vasospasm. Finally, the vascular anatomy of the dog lends itself to a more targeted arterial embolization (compared with the porcine

model, where the vascular rete formation prevents directed embolization).

Given the increasingly important role of MR perfusion and diffusion imaging in understanding the pathophysiology of stroke, this model has been designed to be completely MR imaging-compatible. We have tested this model in both 1.5T and 3T clinical MR imaging scanners. We hypothesize that MR imaging can be successfully used to monitor and guide thrombolysis in real time. A secondary objective is to measure quantitative cerebral blood flow (qCBF) in a well-controlled stroke model with the use of a recently reported method for absolute quantification of cerebral perfusion using MR imaging.¹¹

Materials and Methods

We have developed a canine model of embolic stroke by the catheter-directed injection of autologous blood clots into the internal carotid artery (ICA) that is reversible via intraarterial administration of recombinant tissue plasminogen activator (rtPA) administration. Autologous blood clots were injected directly into the intracranial vasculature via an angiographic catheter to create physiologically “accurate” strokes. Occlusion of the ipsilateral middle cerebral artery (MCA) was confirmed and documented using digital subtraction angiography (DSA). The perfusion defect and evolution of the infarct were evaluated with serial MR perfusion and diffusion imaging. After thrombolysis, additional perfusion and diffusion images were acquired to evaluate the outcome of the treatment.

Animal Preparation

Animal studies were conducted under the guidelines of the local Animal Care and Use Committee (ACUC). All animals were housed indoors under standardized conditions. The dogs were fasted with full access to water for 8 hours before the procedure to minimize anesthesia complications. Six adult dogs (weight = 21.03 ± 2.31 [mean \pm SD]) were preanesthetized with an injection of Innovar (1-mL intramuscular injection) before being transported to our imaging facility. A vein in the foreleg was cannulated (20–22-gauge) for venous access. Anesthesia was induced with propofol (5–7.5 mg/kg intravenous

Received August 15, 2005; accepted after revision December 6.

From the Departments of Radiology (A.S., S. Khawar, B.S., S. Kakodkar, T.J.C., M.R.) and Biomedical Engineering (W.S., T.A.C., T.J.C.), Northwestern University, Chicago, Ill.

Address correspondence to Timothy J. Carroll, PhD, Northwestern University, Department of Radiology, 676 N St. Clair, Suite 1400, Chicago, IL 60611; e-mail: t-carroll@northwestern.edu

[IV]) and maintained by mechanical ventilation with isoflurane (1.5%–2.5%) and 100% oxygen after endotracheal intubation. (Omni-Trak 3100; In Vivo Research, Orlando, Fla). Each dog remained under general anesthesia for the duration of the experiment. The head, neck, and torso of each animal were immobilized with a vacuum immobilizer (VAC-FIX; S&S Par Scientific, Houston, Tex) on the digital angiography table, and the subjects were covered by a heating blanket to maintain body temperature (99.5–102.5°F). Throughout the experiments, continuous monitoring (Millennia 3500; In Vivo Research) of the animal's temperature, heart rate, electrocardiogram, respiration, blood pressure, oxygen saturation level (tongue pulse oximetry), and end tidal CO₂ (34–38 mm Hg) allowed real-time assessment of the physiologic status of the animal.

Magnetic field inhomogeneity artifacts in the vicinity of tissue-air interfaces, such as the sinuses, result in large areas of signal intensity dropout in MR perfusion images. The artifactual signal intensity loss is exacerbated in this stroke model because of the size and location of the frontal sinuses relative to the location of the brain. To alleviate the magnetic susceptibility artifact caused by the paranasal sinuses, bilateral burr holes were drilled, and the frontal sinuses were filled with a viscous material (Surgilube) mixed with trace amounts of barium powder. The barium powder provided attenuation for X-ray guidance of the procedure.

The right common femoral artery was cannulated percutaneously under sonography guidance using a micropuncture set (Cook, Bloomington, Ind), and a 6F arterial sheath was inserted, allowing a 5F catheter to be advanced over a guidewire into one of the ICAs. The arterial sheath was secured in place with sutures (Ethilon 2.0). Left common femoral artery access was gained in a similar fashion, and a 5F pigtail catheter was advanced through a 6F sheath and placed into the left atrium of the heart for injection of the contrast agent required for MR imaging perfusion scans. All catheters and sheaths were periodically flushed with heparinized normal saline (2 U/mL). DSA was performed in the anteroposterior, lateral, and oblique planes to visualize the intracranial vasculature and obtain baseline angiograms.

Preparation of Autologous Clots

After placement of the sheaths, arterial blood was drawn and used to form the blood clot. Four to 10 mL of blood were aspirated and immediately mixed with 0.6 mL (1000 IU/mL) of bovine thrombin (Thrombin-JIMIR; GenTrac, Middleton, Wis). This mixture was then injected into 5 5F straight-tip catheters that were maintained at room temperature for approximately 45 minutes. The threadlike clots were removed and placed in a Petri dish containing phosphate-buffered saline (PBS), were washed several times with PBS to remove nonclotted blood, and transferred into a second Petri dish containing PBS. Clots with high fibrin content (whitish) were transferred into a dish containing an equal mixture suspension of albumin and PBS and drawn into a syringe. The syringe was attached directly to the catheter placed in the ICA and the clots were injected with a gentle rotating action on the plunger. A confirmatory DSA was performed to document the presence and site of the arterial vessel occlusion.

The time of the injection of the clot was documented, and the animals were transported to the MR imaging suite. The vacuum fixation ensured that the catheters did not move or become dislodged during animal transport.

A total of 6 dogs were studied; in 5 of the 6, a thrombus was injected to cause an occlusion of the ipsilateral MCA and a stroke. In 1 study, which served as a control, the dog was fully instrumented with catheters, but no clot was injected. One of the dogs in which a

Table 1: MR imaging protocol

| | Perfusion Weighted* | Diffusion Weighted* |
|------------------------------|---------------------|---------------------|
| TR (ms) | 1150† (1200) | 3000 (1600) |
| TE (ms) | 52 (52) | 97 (91) |
| Field of view (mm) | 148 × 148 | 148 × 148 |
| Matrix | 128 × 128 | 128 × 128 |
| No. of sections | 9–10 | 15 |
| Thickness (mm) | 5.0 | 5.0 |
| Echo-planar imaging factor | 128 | 128 |
| b value (s/mm ²) | n/a | 0, 500, 1000 |
| Bandwidth (Hz/pixel) | 1260 | 1220 |

* Values of the 1.5T experimental are shown in parentheses.

† Fifty phases acquired.

stroke was induced was studied using a 1.5 T scanner, but the remaining experiments were performed using a 3T scanner. Three dogs, all of which were scanned on the 3T MR imaging scanner, were treated with rtPA.

MR Imaging Studies

Five dogs were placed supine head first in a 3T whole-body scanner (Trio; Siemens Medical Solutions, Erlangen, Germany) using an 8-channel, receive-only head coil (Siemens Medical Solutions) for signal intensity reception. A sixth dog was scanned in a 1.5T whole-body MR imaging scanner (Sonata; Siemens Medical Solutions) to provide a baseline measurement for comparison with our high field imaging results. In the experiment performed at 1.5T, a single-channel birdcage coil was used because an 8-channel head coil was not available at the time. The MR imaging protocol consisted of anatomic imaging (T1; T2; fluid-attenuated inversion recovery and 3D T1-weighted, magnetization-prepared rapid acquisition of gradient-echo acquisitions) as well as serial perfusion- (PWI) and diffusion-weighted images (DWI) (Table 1). The perfusion imaging protocol included the acquisition of preinjection and postinjection T1 maps.^{12–14} The changes in T1 resulting from the injection of gadolinium were used to quantify cerebral perfusion after correcting for water exchange effects.^{11,15}

Serial DWI/PWI images were acquired at 30-minute intervals to track the evolution of diffusion changes in the region affected by the stroke and to detect any perfusion changes in response to treatment. The DWI parameters were adapted from the standard clinical protocol used at our site. Because of anatomic differences between humans and dogs, the DWI/PWI images were acquired in the coronal plane. The parameters for the DWI images were: repetition time (TR)/echo time (TE) = 3000/97 ms, bandwidth (BW) = 1220 Hz/pixel, field of view (FOV) = 148 × 148 cm, b-values = 0, 500, 1000 s/mm², matrix = 128 × 128, 15 5-mm sections were acquired with no skip between sections.

The PWI images were colocalized to the central sections of the diffusion images using the scanner's scan prescription tools. The PWI scans were adapted from the clinical protocol used at our site (2D, gradient-echo echo-planar imaging (EPI), TR/TE = 1150/52 ms, BW = 1260 Hz/pixel, 9–10 5-mm sections, 50 phases). For perfusion images, 0.1 mmol/kg body weight of a gadolinium-based contrast agent (Magnevist; Berlex, Princeton, NJ) was injected at 2.0 mL/s through the catheter placed in the left atrium, followed by a saline injection (15 mL at 2 mL/s) to flush the line.

In 3 dogs, chemical thrombolysis of the clot was attempted by intraarterial injection into the catheter placed in the ICA. Thrombolytic therapy was performed using a 2-mg bolus injection of rtPA

(Activase; Genentech, South San Francisco, Calif), followed by a 6-mg infusion performed over 45 minutes. Upon completion of the rtPA infusion, a final DWI/PWI image set was acquired. The dogs were euthanized.

Image Analysis

During the imaging experiments, the stroke and its location were determined based on diffusion and perfusion changes using parametric images that were available from the scanner's processing tools. The prolongation of the time to peak contrast enhancement (TTP) and the mean apparent diffusion coefficient values for the infarct region were evaluated 2 hours 30 minutes after the onset of stroke.¹⁶ The stroke region was defined as hyperintense on TTP images and a 0.2-cm² region of interest (ROI) was placed to cover the corresponding region on the ADC map. The ADC in the normal contralateral brain parenchyma was measured on the same section of the ADC map to serve as an internal control. Mean ADC and SDs were recorded from the normal and contralateral ROI. A Student *t* test, with significance defined at the 5% level, was used to determine whether significant differences in ADCs existed.

Images were analyzed using an off-line workstation to calculate quantitative perfusion images: quantitative cerebral blood volume (qCBV), quantitative cerebral blood flow (qCBF), and mean transit time, using, a recently reported "bookend technique" for perfusion quantification.^{11,15} qCBF was measured in the stroke region and in the normal contralateral region using ROI. ROIs were placed in the normal contralateral region in such a manner as to ensure that the ROI would sample the same proportion of gray/white matter.

The overwhelming signal intensity from cortical vessels is a known source of inaccuracy in MR perfusion images.¹⁷ To limit the effect from these vessels in the qCBF calculation, a previously reported technique for removing the so-called "arterial shinethrough" was implemented.¹⁸ In short, relative CBV images were used to form an arterial mask that included all voxels with a relative CBV value of 30% or greater than an arterial reference signal intensity. The arterial reference signal intensity was determined by placing an ROI to cover the carotid artery or jugular vein, depending on which was more conspicuous in the perfusion images.

The mean values and SDs of qCBF in the ROIs were reported. The 1.5T and 3T results were pooled, and significance differences were determined using a paired *t* test, with significance determined at the 5% level.

Results

Strokes were confirmed in the 5 experiments in which autologous thrombus was injected. In the control experiment, no evidence of stroke was observed on the MR perfusion or diffusion images. A summary of the experimental conditions is shown in Table 2. Figure 1 shows an example of a confirmatory angiogram. In the preinjection angiogram (Fig 1A), the ICA, MCA, and anterior cerebral artery are clearly demonstrated. After the injection of the thrombus, the MCA and its distal branches were absent (Fig 1B), indicating occlusion.

In Fig 2, coronal DWI (*b* = 1000) and ADC images acquired within the first hour after occlusion of the MCA are on the left. The simultaneous increase of diffusion contrast in the *b* = 1000 images, and the reduction of the ADC reflects the increasing water restriction in the infarcted tissue resulting from cytotoxic edema. The regions of prolonged TTP and reduced rCBF correlate well with the abnormalities observed on

Table 2: Experimental conditions

| Description | Stroke Region (mL/100 g/min) | Normal Contralateral (mL/100 g/min) |
|----------------|------------------------------|-------------------------------------|
| 3T, stroke | 2.72 ± 1.21 | 42.93 ± 16.70 |
| 3T stroke*,† | 15.09 ± 4.71 | 49.56 ± 12.75 |
| 3T, stroke* | 3.81 ± 3.77 | 46.51 ± 11.68 |
| 3T stroke* | 6.22 ± 3.96 | 27.42 ± 10.67 |
| 1.5T, stroke | 8.28 ± 2.31 | 44.83 ± 8.08 |
| Mean value | 7.22 ± 4.90 | 42.25 ± 8.64 |
| <i>P</i> value | | <.0007 |
| 3T, control | 51.84 ± 13.26 | 59.50 ± 14.48 |

* Treated with recombinant tissue plasminogen activator.

† Recanalization was observed.

the DWI (*b* = 1000) and ADC images. We found the mean value of ADC in the hypoperfused/diffusion restricted region (ADC = 53.49 ± 12.52 s/mm² [mean ± SD]) to be significantly different (*P* < .05) than the normal contralateral values (ADC = 80.40 ± 8.56 seconds/mm²).

ROI analysis of the stroke and contralateral normal parenchyma are shown in Table 2. The mean values for qCBF in the stroke and contralateral normal ROIs were 7.22 ± 4.90 mL/100 g-min (mean ± SD) and 42.25 ± 8.64 mL/100 g-min, respectively. These differences were found to be statistically significant (*P* < .0007) (Fig 3).

In 3 experiments, we attempted chemical thrombolysis. Recanalization, defined as the restoration of blood flow to the affected area, was observed in 1 case. Figure 4 demonstrates the pretreatment and posttreatment images in the experiment in which recanalization was observed. Figure 4A shows prolonged TTP in the affected region with concomitant reduced ADC in the same region (Fig 4B) in images acquired 2 hours post ictus. After treatment, the region demonstrating prolonged TTP was reduced in volume (Fig 4C), indicating restored perfusion pressure in that region. Postprocessed images of qCBF calculated from the images before and after administration of rtPA show that perfusion has improved in the stroke region (Fig 4E, -F, respectively).

Discussion

We have successfully implemented a model of reversible embolic stroke that is fully MR imaging-compatible. This model has the potential to provide information on the pathophysiology of stroke related to water diffusion and blood flow changes that occur within the first few hours of stroke onset. Furthermore, the use of autologous clots, rather than balloon occlusion or use of a synthetic embolic agent, creates a model that is more amenable for the study of chemical or mechanical thrombolysis. We have seen the potential to track the physiologic response to therapy in real time.

We have measured changes in cerebral blood flow and diffusion changes in "near real time" using standard MR imaging scanners. These images are generated upon scan completion and provide immediate feedback on the status of the tissue at risk. We have been successful in all attempts to create a stroke. The location of the strokes was confirmed with x-ray angiography and the flow distributions further elucidated by MR imaging perfusion/diffusion changes. In the initial PWI/DWI scans, acquired 30 minutes after the injection of the clot, we saw slight differences in DWI (*b* = 1000) and ADC images. As

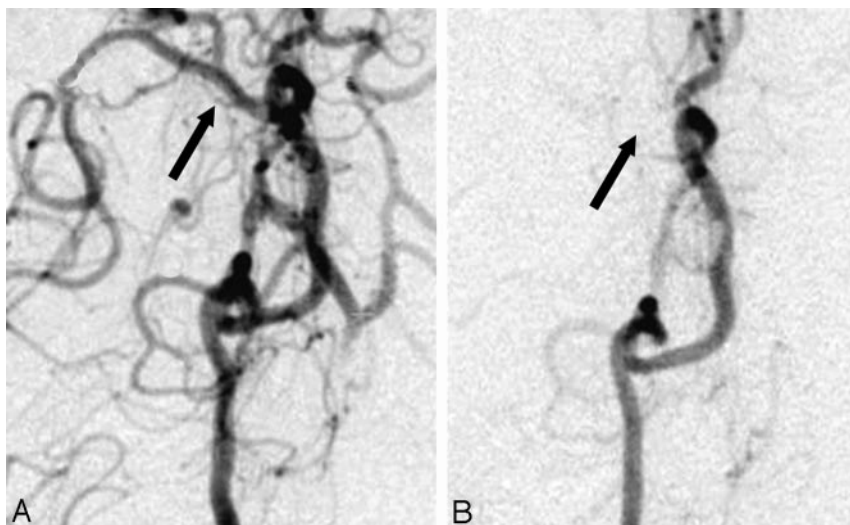


Fig 1. Right internal carotid artery injection delineating the canine circle of Willis (A) before and (B) after injection of an autologous blood clot. Note the conspicuous absence of the middle cerebral artery on the right side after the injection confirming the stroke.

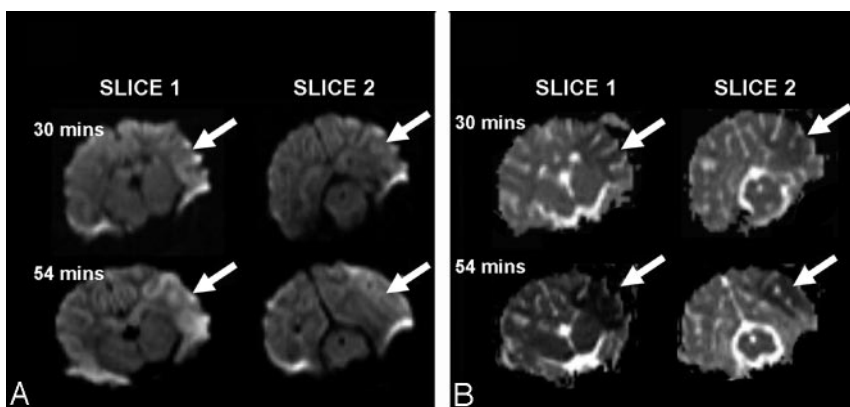


Fig 2. The evolution of the stroke as demonstrated by water diffusion changes in 2 coronal sections acquired in the first hour post ictus. *b* = 1000 images (A) and ADC images (B) demonstrate the increased diffusion contrast and reduced ADC in the region affected by the stroke (arrows).

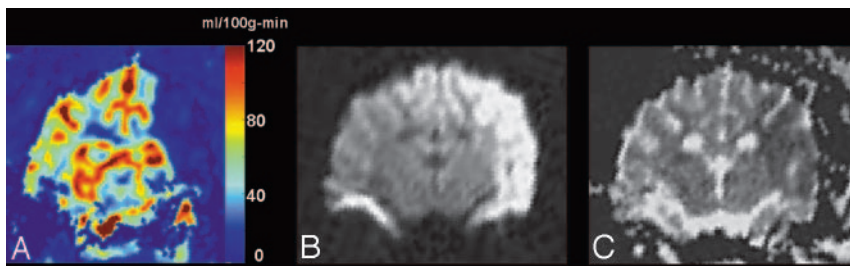


Fig 3. A, An image of quantitative CBF acquired 30 minutes post ictus demonstrates a large region of hypoperfusion ($qCBF < 10$ mL/100 g-min) in the left MCA territory. B, Diffusion-weighted images (*b* = 1000) acquired after 2 hours show that, in this case, the territory of hypoperfusion observed immediately after the stroke goes on to become a pronounced diffusion abnormality. C, ADC values confirm the region of diffusion seen in the *b* = 1000 image.

the stroke evolved, we were able to observe the increase in the hyperintensity on the *b* = 1000 images and a corresponding decrease in the ADC values (Fig 2). For the final time point that was acquired 2 hours postictally, we have found statistically significant differences in both ADC and *qCBF* in the regions affect by the stroke.¹⁶

The model we have developed has been designed to be MR imaging-compatible so that imaging tools can be used to track the development of physiologic changes that occur as a result of the stroke. Our earliest attempts at this model were confounded by large signal intensity voids in the vicinity of the frontal sinuses of the dogs. These signal intensity dropouts were most pronounced in the gradient-echo EPI acquisitions used for the PWI bolus tracking. The location and size of the artifacts were worsened by the fact that we were using a high-field MR imaging scanner. To circumvent the problem of the field inhomogeneity, we filled the sinus with Surgilube to reduce the local field inhomogeneity. This approach allowed

many more artifact-free sections to be acquired. In our studies, 9–10 sections were acquired, whereas examinations performed without filling the sinuses yielded only 2–3 usable sections. Furthermore, these sections were from the more posterior portion of the brain, making selection of the arterial input function in the MCA nearly impossible. We mixed small amounts of barium powder with the Surgilube to render it radiopaque. The opacity of the Surgilube gel allowed the interventionist to view the filling of the sinuses under x-ray guidance. Both lateral and coronal x-ray projections were acquired to ensure complete filling of the sinuses.

In our model, x-ray DSA was required both to guide the catheters for thrombus deposition and confirm MCA occlusion. To perform the MR imaging, the animal must be transported to the MR imaging scanner. The transport of the animal between the angiography suite and the MR scanner is complex and requires the coordination of several elements. It is hoped in the future that many of these steps can be elimi-

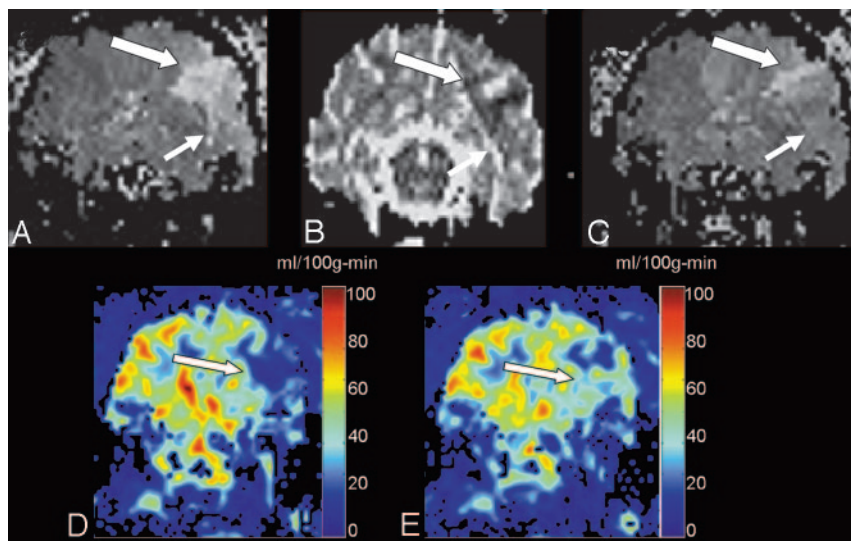


Fig 4. Thrombolysis achieved partial restoration of cerebral perfusion in 1 animal.

A, Pretreatment time to peak of a single coronal section demonstrates a large region of prolonged TTP in the left MCA territory (arrows).

B, The ADC image acquired at 2 hours confirms a region of reduced ADC.

C, The corresponding TTP acquired upon completion of the infusion of rtPA shows marked improvement of flow in the affected territory. Quantitative flow images calculated before (*D*) and after (*E*) treatment show that qCBF in the region affected by the stroke has been restored to a value that is above the known threshold for ischemic stroke.

nated through the use of a combined x-ray/MR imaging scanner.

The development of a full array of MR imaging catheter tracking tools that would eliminate the need of the x-ray machine would also be desirable, and several groups are actively working in this area.^{19–22} When these tools are perfected, it is hoped that both intravenous and intraarterial MR-guided thrombolysis can be developed and evaluated for the eventual use in humans.

We successfully re-established flow in 1 of 3 dogs that were treated with rtPA. This rate is rather low for these initial experiments, and we believe this rate may reflect some shortcomings in the animal model. For example, we terminated the experiments upon completion of the rtPA infusion. In our protocol, the rtPA was infused as a bolus plus an infusion that lasted 45 minutes; therefore, in all cases, the last MR imaging that was performed was within 1 hour of the beginning of the rtPA infusion. This may have prevented the observation of flow restoration occurring in a more delayed fashion. Second, the volume of thrombus injected was not standardized between experiments. In future studies, we will explore whether a smaller clot burden would lyse more quickly and completely.

We have applied a previously reported technique for quantification of CBF. In these experiments our average qCBF value in the unaffected region was in good agreement with previously published canine values.²³ One difficulty in the use of the canine model is the relative paucity of white matter compared with the human brain. White matter has a lower metabolic demand, and therefore is perfused at roughly half the rate for gray matter. This has important consequences for the extrapolation of these data to humans. Because thresholds for cell death can potentially depend on metabolic need, the limited amount of white matter in dogs should be considered. What may be of particular interest in further experiments is the relation between the level of hypoperfusion as measured with qCBF and the recanalization rate. In the second experiment, where we observed restoration of flow, the baseline qCBF in the stroke region, though hypoperfused, was 3 times the mean value of the other dogs (roughly 4 SDs).

This study was not without limitations. First and foremost, we did not control for the volume of the blood clot that was

injected. In future studies, we will determine the relation between clot burden, the degree of hypoperfusion, and the recanalization rate. This underlines the goal of this work: to create a reproducible model of embolic stroke for well-controlled experiments. In this study we have not compared our qCBF measurements with an established standard of reference, such as colored microsphere deposition.^{24,25} This will be the aim of future studies on our models.

Conclusion

Our study results indicate that we have developed a reproducible canine model of thromboembolic stroke that is MR imaging-compatible. Using this model, we were able to track the evolution of perfusion and diffusion changes and assess the response to MR-guided thrombolytic therapy. We measured qCBF and showed that the values obtained were in close agreement with published values in a canine model. We compared qCBF in the normal and hypoperfused regions and showed that these values were significantly different.

References

1. American Heart Association. **Heart disease and stroke statistics—update 1995**. Dallas, Tex: American Heart Association; 1995.
2. Broderick J, Brott T, Kothari R, et al. **The Greater Cincinnati/Northern Kentucky Stroke Study: preliminary first-ever and total incidence rates of stroke among blacks**. *Stroke* 1998;29:415–21.
3. Anonymous. **Tissue plasminogen activator for acute ischemic stroke**. The National Institute of Neurological Disorders and Stroke rt-PA Stroke Study Group. *N Engl J Med* 1995;333:1581–87.
4. IMS Study Investigators. **Combined intravenous and intra-arterial recanalization for acute ischemic stroke: the Interventional Management of Stroke Study**. *Stroke* 2004;35:904–11.
5. del Zoppo GJ, Higashida RT, Furlan AJ, et al. **PROACT: a phase II randomized trial of recombinant pro-urokinase by direct arterial delivery in acute middle cerebral artery stroke**. PROACT Investigators. *Prolyse in Acute Cerebral Thromboembolism*. *Stroke* 1998;29:4–11.
6. Kase CS, Furlan AJ, Wechsler LR, et al. **Cerebral hemorrhage after intra-arterial thrombolysis for ischemic stroke: the PROACT II trial**. *Neurology* 2001;57:1603–10.
7. Katzan IL, Hammer MD, Hixson ED, et al. **Use of tissue-type plasminogen activator for acute ischemic stroke: the Cleveland area experience**. *JAMA* 2000;283:1151–58.
8. Chiu D, Krieger D, Villar-Cordova C, et al. **Intravenous tissue plasminogen activator for acute ischemic stroke: feasibility, safety, and efficacy in the first year of clinical practice**. *Stroke* 1998;29:18–22.
9. Nabavi DG, Cenic A, Dool J, et al. **Quantitative assessment of cerebral hemo-**

- dynamics using CT: stability, accuracy, and precision studies in dogs. *J Comput Assist Tomogr* 1999;23:506–15
10. Ryder RC, Sevick RJ, Morrish WF, et al. **Development and evaluation of a reversible embolic stroke model for MR endovascular thrombolysis.** In: *Proceedings of the International Society for Magnetic Resonance in Medicine*. Berkeley, Calif: International Society for Magnetic Resonance in Medicine; 2003:1193. Available at: <http://cds.ismrm.org/ismrm-2003/1193.pdf>
 11. Sakaie KE, Shin W, Curtin KR, et al. **Methods for improving the accuracy of quantitative cerebral perfusion imaging.** *J Magn Reson Imaging* 2005;21:512–19
 12. Schwarzbauer C, Syha J, Haase A. **Quantification of regional blood volumes by rapid T1 mapping.** *Magn Reson Med* 1993;29:709–12
 13. Kuppusamy K, Lin W, Cizek GR, et al. **In vivo regional cerebral blood volume: quantitative assessment with 3D T1-weighted pre- and postcontrast MR imaging.** *Radiology* 1996;201:106–12
 14. Sakaie KE, Shin W, Carroll TJ. **Comparison of analysis methods for measuring T1 by trueFISP readout of inversion recovery.** In: *Proceedings of the International Society for Magnetic Resonance in Medicine*. Berkeley, Calif: International Society for Magnetic Resonance in Medicine; 2004:2118.
 15. Shin W, Cashen TA, Horowitz SW, et al. **Quantitative CBV measurement from static T1 changes in tissue and correction for intravascular water exchange.** *Magn Reson Med* 2006;56:138–45.
 16. Marks MP, Tong DC, Beaulieu C, et al. **Evaluation of early reperfusion and i.v. tPA therapy using diffusion- and perfusion-weighted MRI.** *Neurology* 1999;52:1792–98
 17. Carroll TJ, Haughton VM, Rowley HA, et al. **Confounding effect of large vessels on MR perfusion images analyzed with independent component analysis.** *AJNR Am J Neuroradiol* 2002;23:1007–12
 18. Carroll TJ, Teneggi V, Jobin M, et al. **Absolute quantification of cerebral blood flow with magnetic resonance, reproducibility of the method, and comparison with H2(15)O positron emission tomography.** *J Cereb Blood Flow Metab* 2002;22:1149–56
 19. Quick HH, Kuehl H, Kaiser G, et al. **Interventional MRA using actively visualized catheters, TrueFISP, and real-time image fusion.** *Magn Reson Med* 2003;49:129–37
 20. Quick HH, Zenge MO, Kuehl H, et al. **Interventional magnetic resonance angiography with no strings attached: wireless active catheter visualization.** *Magn Reson Med* 2005;53:446–55
 21. Omary RA, Green JD, Fang WS, et al. **Use of internal coils for independent and direct MR imaging-guided endovascular device tracking.** *J Vasc Interv Radiol* 2003;14(2 Pt 1):247–54
 22. Green JD, Omary RA, Finn JP, et al. **Passive catheter tracking using MRI: comparison of conventional and magnetization-prepared FLASH.** *J Magn Reson Imaging* 2002;16:104–09
 23. Nabavi DG, Cenic A, Craen RA, et al. **CT assessment of cerebral perfusion: experimental validation and initial clinical experience.** *Radiology* 1999;213:141–49
 24. Prinzen FW, Bassingthwaite JB. **Blood flow distributions by microsphere deposition methods.** *Cardiovasc Res* 2000;45:13–21
 25. Ahmed J, Pulfer MK, Linsenmeier RA. **Measurement of blood flow through the retinal circulation of the cat during normoxia and hypoxemia using fluorescent microspheres.** *Microvasc Res* 2001;62:143–53